have reported an electrical resonance in hair cells of the terrapin cochlea. Whether this mechanism exists in other cochleas is not yet known.
3. S. M. Khanna and D. G. B. Leonard, *Science* **215**, 305 (1982); P. M. Sellick, R. Patuzzi, B. M. Johnstone, *J. Acoust. Soc. Am.* **72**, 131 (1982).
4. T. F. Weiss *et al.*, *J. Acoust. Soc. Am.* **70**, S50 (1981).
5. T. F. Weiss, W. T. Peake, A. Ling, T. Holton, in *Evoked Electrical Activity in the Auditory Nervous System*, R. F. Naunton and C. Fernandez, Eds. (Academic Press, New York, 1978), p. 91.
6. T. F. Weiss, M. J. Mulroy, R. G. Turner, C. L. Pike, *Brain Res.* **115**, 71 (1976).
7. T. Holton and T. F. Weiss, *J. Physiol. (London)*, in press.
8. W. T. Peake and A. L. Ling, *J. Acoust. Soc. Am.* **67**, 1736 (1980).
9. L. S. Frishkopf, D. J. DeRosier, E. H. Egelman, *Soc. Neurosci. Abstr.* **8**, 40 (1982); T. Holton and A. J. Hudspeth, *ibid.*, p. 40; T. Holton, *Assoc. Res. Otolaryngol. Abstr.* **6**, 98 (1983).
10. M. J. Mulroy, *Brain Behav. Evol.* **10**, 69 (1974).
11. Pivoting of the stereocilia has been observed in hair cells of the frog crista in response to direct mechanical displacement [A. Flock, in *Psychophysics and Physiology of Hearing*, E. F. Evans and J. P. Wilson, Eds. (Academic Press, London, 1977), p. 15].
12. A. J. Hudspeth and D. P. Corey, *Proc. Natl. Acad. Sci. U.S.A.* **74**, 2407 (1977).
13. The amplitudes of angular displacement of the hair bundles shown in Fig. 3 do not exceed ±0.04 rad (±2.3°). From the geometry of the organ, the assumption that the organ pivots about the neural limbus, and the basilar-membrane data in the intact preparation (*8*), we estimate that sounds producing equivalent motions in the intact animal would not exceed 100-dB sound-pressure level at the eardrum.
14. There are at least two reasons somatic motion measured by the video technique demonstrates frequency-dependent place organization while basilar membrane motion measured by the Mössbauer technique in the intact preparation (*8*) does not. (i) The video measurements are made at the top (somatic) surface of the organ, whereas the Mössbauer measurements are made at the bottom (basilar-membrane) surface. Since these two surfaces are separated by the 50-μm thickness of the papilla, their motions need not necessarily show the same dependence on frequency and place. (ii) The two measurement techniques resolve motion along orthogonal axes. The video technique measures side-to-side motion of the organ, in a plane of focus parallel to the basilar membrane; the Mössbauer technique usually measures up-and-down motion of the basilar membrane, and thus will not resolve any side-to-side components of basilar membrane motion that result from the organ's pivoting about the limbus.
15. In fish [R. R. Fay and A. N. Popper, in *Comparative Studies of Hearing in Vertebrates*, A. N. Popper and R. R. Fay, Eds. (Springer-Verlag, New York, 1980), p. 3], amphibians [E. R. Lewis, *Neurosci. Lett.* **21**, 131 (1981)], reptiles [(*10*); R. G. Turner, A. A. Muraski, D. W. Nielsen, *Science* **213**, 1519 (1981)], birds [C. A. Smith, in *Progress in Sensory Physiology*, D. Ottoson, Ed. (Springer-Verlag, New York, 1981), vol. 2, p. 135], and mammals [D. J. Lim, *J. Acoust. Soc. Am.* **67**, 1686 (1980)].
16. Although micromechanical tuning has not been measured directly in any mammalian cochlea, recent measurements of a sharply selective, physiologically vulnerable component of basilar membrane motion (*3*) and of cochlear acoustic distortion products [D. T. Kemp, *J. Acoust. Soc. Am.* **64**, 1386 (1978); S. D. Anderson and D. T. Kemp, *Arch. Otorhinolaryngol.* **224**, 47 (1979); D. O. Kim, *Hearing Res.* **2**, 297 (1980)] have been interpreted as suggesting the existence of micromechanical processes coupled into the motion of the basilar membrane.
17. S. L. Shotwell, R. Jacobs, A. J. Hudspeth, *Ann. N.Y. Acad. Sci.* **374**, 1 (1981).
18. Supported by fellowships to T.H. from the Del E. Webb Foundation and the National Institutes of Health (GM07301) and grants to A.J.H. from NIH (NS13154) and the System Development Foundation. We thank J. N. Power for electronic design and construction, R. Jacobs for technical assistance, and H. Berg, R. A. Eatock, M. Konishi, R. S. Lewis, and D. C. Van Essen for comments on the manuscript.
* Requests for reprints should be addressed to Department of Physiology, University of California School of Medicine, San Francisco 94143.

28 February 1983; accepted 25 July 1983

Alternating Current Delivered into the Scala Media Alters Sound Pressure at the Eardrum

Abstract. *Alternating current delivered into the scala media of the gerbil cochlea modulates the amplitude of a test tone measured near the eardrum. Variations in the electromechanical effect with acoustic stimulus parameters and observed physiological vulnerability suggest that cochlear hair cells are the biophysical origin of the process. Cochlear hair cells have traditionally been thought of as passive receptor cells, but they may play an active role in cochlear micromechanics.*

The cochlea functions as a mechanical frequency analyzer with a continuous distribution of resonant frequencies along its length. The frequency response of the vibration of the basilar membrane, upon which sensory cells (hair cells) are located, has been studied extensively (*1–3*). Recent measurements indicate that the frequency selectivity of the basilar membrane is sufficient to account for the sharp frequency tuning observed in cochlear inner hair cells and auditory nerve fibers (*2*).

Rhode demonstrated the physiological vulnerability of cochlear mechanics in the squirrel monkey and showed that the frequency selectivity and relative sensitivity decreased at high sound-pressure levels (SPL's) (*3*). His work has been extended to the cat and guinea pig (*2*). Cochlear mechanics can be modified by stimulation of efferent fibers that are thought to synapse primarily on outer hair cells (*4, 5*). The mechanics can also be modified by changes in the cochlear endolymphatic potential, which is the voltage gradient across the sensory epithelium (*4*).

Several proposed models assume an active mechanical role for the hair cells in the generation of the sharply tuned basilar membrane response (*6, 7*). Because the stereocilia of the outer hair cells are embedded in the tectorial membrane overhanging the basilar membrane (*8*), the models generally consist of a resonant basilar membrane coupled to the tectorial membrane by force-generating hair cells. The hair-cell stereocilia have been suggested to produce a force proportional to either displacement (*7*) or velocity (*6*). Both classes of models are prone to instability, which could account for a type of objective tinnitus in which sound is radiated out of the ear. If either class of models is valid, the hair cells must be able to undergo mechanical changes very rapidly.

We now report an electromechanical phenomenon in the cochlea, with characteristics consistent with the hypothesized hair-cell force-generating mechanism. By passing sinusoidal electrical currents into the scala media of the cochlea, we can induce rapid mechanical changes. The effect seems to be related to the hair-cell receptor potential, as reflected in the cochlear microphonic (CM).

Healthy gerbils weighing 60 to 90 g were anesthetized with sodium pentobarbital. A calibrated, closed acoustic system consisting of an earphone and probe-microphone was cemented into place at the meatal entrance to the bulla. A 0.16 or 1.0*M* KCl-filled glass pipette with a tip diameter of approximately 5 μm was inserted into the scala media of either the first or second cochlear turn, and sinusoidal currents of 1 to 50 μA peak-to-peak were delivered by an isolated current source. A subcutaneous, Ag-AgCl current return electrode was placed in the neck. The entire stimulus and data-collection system was controlled by computer.

Single tones were delivered to the earphone, and the resulting sound pressure near the tympanic membrane was measured with a probe-tube microphone. The amplified microphone output was sampled by an analog-to-digital converter at a rate of eight samples per period of the acoustic stimulus. Multiple data records of 1024 points were averaged and stored for subsequent Fourier analysis.

Figure 1A shows a typical spectrum obtained through the use of a 800-Hz tone at 65 dB SPL with a delivered current of 25 μA peak-to-peak at 150 Hz. The signal component at acoustic frequency F_a is the primary tone delivered to the earphone. The second and third acoustic harmonics are at multiples of F_a. There exist acoustic emissions at the frequency of the electrical stimulation (F_e) and its second harmonic. The spectral components of interest are those separated from the primary signal and its harmonics by a distance equal to F_e. We refer to these components as the upper

and lower sidebands since they resemble the sidebands of modulation theory. Values of F_e below 1 kHz are generally most effective in generating the sidebands, but we have observed sidebands with frequencies as high as 3 kHz (*9*). The sidebands are always measurable in preparations showing good cochlear microphonic and endolymphatic potential, but only if the electrode delivering the current is inside the scala media. Figure 1B shows the spectrum after the ear was subjected to a 1-kHz tone at 107 dB SPL for 8 minutes. The sidebands disappeared and the CM was greatly reduced, which suggests loss of hair-cell function due to acoustic trauma.

The magnitude of the sidebands resembles the fundamental component of the CM as plotted against sound level (Fig. 2). Growth at unity slope followed by reduced slope are the salient features of the curves. The CM and sideband curves agree at high acoustic frequencies (Fig. 2C). The similarities between the CM and the sidebands suggest that the mechanical-to-electrical transduction process may affect the generation of the observed acoustic emissions. For frequencies well below the resonant frequency of the electrode location, however, the high-SPL bendover of the sidebands begins at a lower sound level than the CM. In addition, the sidebands can begin to grow again at highest SPL's, while the CM remains saturated (Fig. 2A).

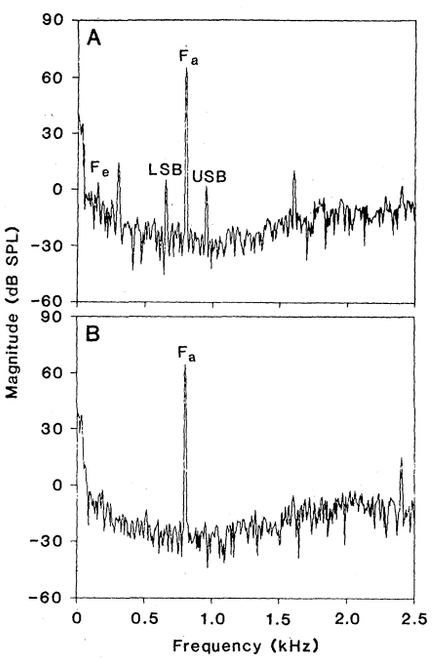

Fig. 1. (A) Acoustic spectrum measured near the eardrum during delivery into the scala media of turn 1 of a 25-μA peak-to-peak current at 150 Hz. The largest component is the tonal input at 800 Hz at 65 dB SPL. The smaller components flanking the 800-Hz component are upper and lower sidebands (*USB* and *LSB*), which indicate modulation of the amplitude of the input tone due to current injection. The component at F_e is an electrically stimulated emission from the ear canal. The second harmonic of this component is larger than the fundamental. (B) Acoustic trauma produced by an 8-minute exposure to a 107-dB SPL sound at 1 kHz reduces the modulation components and the electrically stimulated emission and its harmonic below the noise level.

Acoustic stimuli consisting of two tones at the acoustic and electric frequencies can produce distortion products in the ear canal at the frequencies of the sidebands (*10*). These acoustic distortion products disappear or change in damaged or dead cochleas. Since the sidebands similarly depend on physiological viability, they might have been produced by the current electrode vibrating in the scala media. Indeed, acoustic components exist at the frequency of electrical stimulation and its second harmonic (Fig. 1A) (*11*). These components can be reduced in size after exposure to loud sounds, however, indicating that they too are of physiological origin (Fig. 1B). Moreover, sidebands are related to the electric frequency and not its harmonic, which is the larger of the two acoustic components at the eardrum (*12*). In addition, we have not observed acoustic emissions at the electrical frequency for values of F_e below 150 Hz, and yet these values of F_e produce large sidebands. Thus we conclude that the sideband generation is related to current injection by a physiological, electromechanical effect and not simply a mechanically produced, two-tone effect.

We model the process in terms of electrically induced stiffness changes affecting cochlear mechanics. The acoustic frequencies we used are well below the resonant frequency of the basilar membrane at the current-injection electrode location. In this frequency region, cochlear mechanics are thought to be dominated by the stiffness of the basilar membrane. A digital stimulation of cochlear mechanics (*13*) that includes time-varying, distributed stiffnesses produces qualitative agreement with experimental results. In greatly simplified form, the model produces sideband components due to a sinusoidally varying spring constant in the simulated mechanical system when the system is driven at the acoustic frequency. This process is a form of modulation.

We propose that the model is related to the physiology in the following manner. The stiffness of the basilar membrane is due in part to the stiffness of the hair-cell stereocilia. The presence of actin (*14*) and myosin (*15*) and their arrangement in cochlear hair cells (*16*) gives them their stiffness as well as their assumed electromechanical capability. By passing current through the organ of Corti, we may be dynamically modulating that stiffness. Perhaps the current acts by modulating the intracellular Ca^{2+} concentration, since that concentration alters the stiffness of frog hair-cell stereocilia (*17*). If an ion species effects the dynamic changes we observe, the rapidity of the changes would allow only small diffusion distances for the regulatory ionic species.

The requirement that the current injection electrode be delicately placed in the scala media, the similarity of the sidebands and CM, and the observed physiological vulnerability suggest that the cochlear hair cells are the origin of the

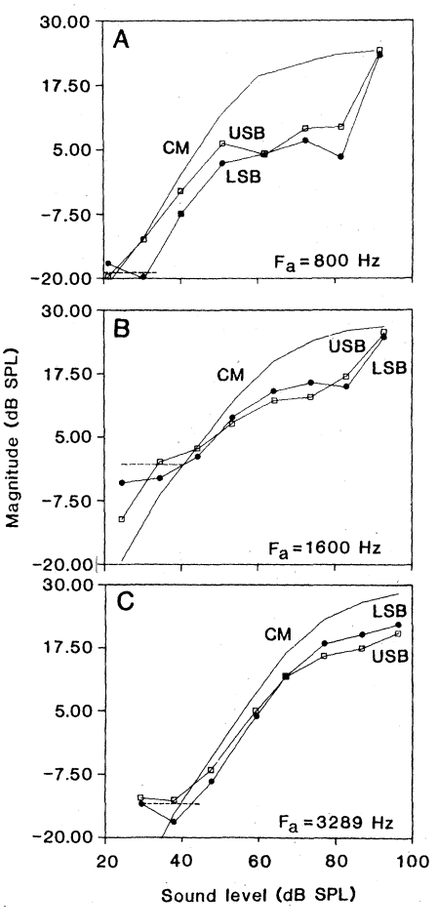

Fig. 2. Magnitudes of the upper and lower sidebands (*USB* and *LSB*) and CM as a function of input tone level at the indicated acoustic frequencies. The electrical current was 25 μA peak-to-peak at 150 Hz. The horizontal broken line indicates the approximate noise level at lower SPL's. The CM is plotted on an arbitrary log scale.

observed electromechanical phenomena and that the transduction process may play an important role. The hypothesis that stereocilia stiffness is modified by current injection is not directly addressed by the data.

ALLYN E. HUBBARD
Department of Electrical, Computer and Systems Engineering, College of Engineering, and *Department of Otolaryngology, School of Medicine, Boston University, Boston, Massachusetts 02215*
DAVID C. MOUNTAIN
Department of Biomedical Engineering, College of Engineering, and *Department of Otolaryngology, School of Medicine, Boston University*

References and Notes

1. G. von Bekesy, *J. Acoust. Soc. Am.* **25**, 770 (1953); B. M. Johnstone and G. K. Yates, *ibid.* **55**, 584 (1974); B. M. Johnstone and A. J. F. Boyle, *Science* **158**, 389 (1967); L. U. E. Kohlloffel, *Acoustica* **27**, 49 (1972).
2. S. M. Khanna and D. G. B. Leonard, *Science* **215**, 305 (1982); P. M. Sellick, R. Patuzzi, B. M. Johnstone, *J. Acoust. Soc. Am.* **72**, 131 (1982).
3. W. S. Rhode, *J. Acoust. Soc. Am.* **49**, 1218 (1971); in *Basic Mechanisms in Hearing*, A. Moller, Ed. (Academic Press, New York, 1973), pp. 49–68.
4. D. C. Mountain, *Science* **210**, 71 (1980).
5. J. H. Siegel and D. O. Kim, *Hearing Res.* **6**, 171 (1982).
6. T. Gold, *Proc. R. Soc. London Ser. B* **135**, 492 (1948); S. T. Neely, thesis, Washington University (1981).
7. D. C. Mountain, *Abstr. Midwinter Res. Meet. Assoc. Res. Otolaryngol.* **5**, 8 (1982).
8. D. J. Lim, *J. Acoust. Soc. Am.* **67**, 1686 (1980).
9. Frequencies as low as 25 Hz produce sidebands. The effect seems to be a low-pass one.
10. For frequencies and levels under consideration, the second tone at the electrical frequency must be on the order of 60-dB SPL to produce distortion products of magnitude comparable to that of the sidebands produced with 25-μA current.
11. D. C. Mountain and A. E. Hubbard, *Abstr. Midwinter Res. Meet. Assoc. Res. Otolaryngol.* **6**, 103 (1983).
12. A current at the second harmonic frequency would be capable of producing sidebands.
13. A. Hubbard, *Model. Simulation* **7**, 1278 (1976).
14. A. Flock and H. C. Cheung, *J. Cell Biol.* **75**, 334 (1977).
15. J. Maccartney, S. Comis, J. Pickles, *Nature (London)* **288**, 491 (1980).
16. M. Itoh and T. Nakaskima, *Acta Otolaryngol.* **90**, 385 (1980); A. Flock, and E. Murray, *ibid.* **83**, 85 (1977); L. G. Tilney, D. J. DeRosier, M. J. Mulroy, *J. Cell Biol.* **86**, 244 (1980).
17. S. Orman and A. Flock, *Soc. Neurosci. Abstr.* **7**, 536 (1981).
18. Supported by grant NS16589 from the National Institutes of Health.

1 March 1983; accepted 12 August 1983

Anti-T-Cell Reagents for Human Bone Marrow Transplantation: Ricin Linked to Three Monoclonal Antibodies

Abstract. *Three new reagents that react against human T cells were synthesized by covalently linking the toxin ricin to monoclonal antibodies recognizing differentiation antigens on the surface of T lymphocytes. Each of these immunotoxins selectively inhibited T-cell proliferation when the cells were incubated in the presence of lactose. Multipotent human stem cells were inhibited only at much higher concentrations. Mixtures of all three immunotoxins were more effective than any one alone. These reagents have the potential for preventing graft-versus-host disease in man.*

Bone marrow transplantation is used as an aggressive therapy for severe and life-threatening hematological disorders such as immunodeficiency diseases (*1*) and leukemia (*2*). Even when donors and recipients are matched with respect to their histocompatibility antigens (HLA), graft-versus-host disease (GVHD) may develop in which immunocompetent T cells in the donor graft react against the recipient's minor HLA antigens. In mice, GVHD can be prevented by eliminating T cells in the donor graft (*3–5*). In man, monoclonal antibodies to T cells have been used to treat donor cells before infusion, but the outcome has been disappointing (*6*). Antibody plus complement or lectin and sheep red blood cell fractionation (*7*) have also been used to deplete bone marrow of T cells. A new approach which is simple, rapid, and highly reproducible is to use conjugates of monoclonal antibody and toxins, which are capable of selectively killing T cells (*8*). These immunotoxins, when incubated with donor marrow in vitro, can protect mice in experimental models of lethal GVHD (*9, 10*). We have synthesized and tested three anti-T-cell immunotoxins that have potential for use in human bone marrow transplantation.

We selected the monoclonal antibodies TA-1, T101, and UCHT1 for our studies. TA-1 is an immunoglobulin G (IgG)2a antibody that binds to greater than 90 percent of peripheral blood T cells and monocytes, and approximately 70 percent of thymocytes when examined by indirect immunofluorescence (*11*). The cell surface molecule recognized by TA-1 is a two-chain, noncovalently linked glycoprotein complex of 170,000 and 95,000 daltons (*12*). TA-1 also recognizes monocytes and large granular lymphocytes with natural killer (NK) cell activity (*13*). Because these cells have been implicated in the pathology of GVHD (*14*), TA-1 was a particularly attractive antibody to link to ricin. T101, an IgG2a antibody, binds to all peripheral blood T cells (*15*). T101 recognizes a 65,000-dalton determinant on immature and mature normal T cells and T-cell lines. UCHT1, an IgG1 antibody, identifies a determinant on all human peripheral T lymphocytes and on a minority of thymocytes (*16*). UCHT1 precipitates the same glycoprotein as OKT3, that is, a complex of approximately 19,000 daltons (*17*). These three monoclonal antibodies were covalently linked to intact ricin by way of a thioether linkage by slight modification of a previously published procedure (*8*).

The plant seed toxin ricin contains two disulfide-linked subunits that have distinct roles in killing cells. The A chain enzymatically inactivates 60*S* ribosomes, inhibiting protein synthesis (*18*). The B chain binds to galactose-containing cell surface receptors (*18*) and increases the rate of A chain transport to ribosomes by an unknown mechanism (*19, 20*). Intact ricin (*8*) and ricin A chain (*20, 21*) linked to antibodies have been shown to specifically kill antigen-bearing cells. Immunotoxins made with ricin often exhibit more cell killing than those made with A chain alone (*10, 20, 22*). Immunotoxins made with intact ricin require the presence of 100 m*M* lactose to block the ricin binding site and thus cannot be used in vivo. Since procedures for bone marrow transplantation permit the treatment of donor cells in vitro, we elected to use the more potent, intact ricin immunotoxins.

The sensitivity of the three immunotoxins to T cells was determined by incubating them at various concentrations with peripheral blood mononuclear cells (PBMC) for 2 hours in the presence of lactose. The cells were then washed and cultured for 3 days in the presence of the T-cell mitogen phytohemagglutinin (PHA). All three immunotoxins—TA-1–ricin, T101-ricin, and UCHT1-ricin—inhibited the PHA response more than 90 percent at 300 ng/ml (Fig. 1).

Stem cells must be preserved in the donor marrow for engraftment to occur in the recipient. Therefore, we examined the selectivity of the immunotoxins for different cell types by determining their toxicity to pluripotential stem cells using the CFU-GEMM assay (colony-forming units, granulocyte, erythroid, monocytic, megakaryocytic) (*23, 24*). Figure 1 shows that the concentration of immunotoxin that inhibits T cells more than 90 percent, 300 ng/ml, does not significantly inhibit the growth of CFU-GEMM. If the doses of immunotoxin that inhibit the PHA response and CFU-GEMM colony formation by 50 percent are compared, it is evident that T101-ricin and UCHT1-